Bimolecular Imaging

DOI: 10.1002/anie.201003761

Readily Accessible Bicyclononynes for Bioorthogonal Labeling and Three-Dimensional Imaging of Living Cells**

*Jan Dommerholt, Samuel Schmidt, Rinske Temming, Linda J. A. Hendriks, Floris P. J. T. Rutjes, Jan C. M. van Hest, Dirk J. Lefeber, Peter Friedl, and Floris L. van Delft**

The advent of chemical biology tools for imaging and tracking of biomolecules (proteins, lipids, glycans) in their native environment is providing unique insights into cellular processes that are not achievable with traditional biochemical or molecular biology tools.[1] Bioorthogonal labeling of biomolecules has proven particularly useful for the detection and study of glycans[2] and lipids,[3] based on a highly selective reaction between an abiotic functional tag and a designed chemical probe. With respect to the abiotic tag, azide has been used extensively because of its straightforward chemical introduction, small size, and relative inertness.[4] The finding that azides react rapidly and cleanly with terminal acetylenes in the presence of copper(I), the quintessential "click" reaction, has found tremendous application in life and material sciences.[5] However, because up to 20 mol% of copper(I) species is typically used, such click chemistry is not suitable for labeling of living systems without compromising cell function.[6] Apart from that, the presence of copper may induce oligonucleotide[7] and polysaccharide[8] degradation. To avoid the use of toxic metals, several metal-free bioorthogonal labeling reaction have been developed.[9] In particular, phosphines have been used for covalent ligation to azides, a procedure known as Staudinger ligation.[10] However, owing to the oxygen sensitivity of phosphines, recent focus of chemical ligation is shifting towards strain-promoted cycloaddition reactions with cyclooctynes (Scheme 1a).[11] Most prominently, azides were find to react with cyclooctynes with high reaction rates in a so-called strain-promoted alkyne–azide cycloaddition (SPAAC).[12] The toolbox of metal-free bioorthogonal reactions was most recently further expanded by our research group[13] and others,[14] by demonstrating that cyclooctynes undergo even more rapid strain-promoted cycloaddition with nitrones (SPANC), a procedure that was found suitable for dual, irreversible, and site-specific N-terminal modification of proteins.[13]

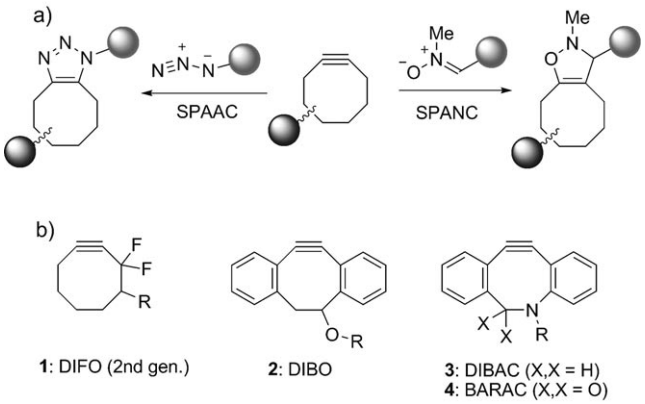

Scheme 1. Reactions and structures of cyclooctyne compounds for strain-promoted cycloaddition. a) Cycloaddition with azide (SPAAC) or nitrone (SPANC). b) Structures of the most commonly employed cyclooctynes.

The broad application of metal-free cycloaddition in life sciences is, however, hampered by the limited commercial availability and lengthy synthetic routes for preparation of the most common cyclooctynes (Scheme 1b). For example, eight synthetic steps are required to generate second-generation DIFO (**1**),[15] nine steps for DIBAC (**3**),[16] and seven steps for BARAC (**4**),[17] while yields are usually low (10% for **2**,[18] 16% for **4**). Additional modifications, such as dibenzoannulation (compounds **2**–**4**), increase lipophilicity and may, therefore lead to non-specific binding to proteins.[17]

Here we report bicyclo[6.1.0]nonyne (BCN) as a novel ring-strained alkyne for metal-free cycloaddition reactions with azides and nitrones. Bicyclononyne derivatives, which were obtained in a highly straightforward process through cyclopropanation of 1,5-cyclooctadiene, are C_s symmetrical and display excellent reaction kinetics in strain-promoted cycloaddition reactions. Functionalized derivatives of BCN were applied in the labeling of proteins and glycans, as well as in the three-dimensional visualization of living melanoma cells.

Based on the known reactivity enhancement of cyclopropane fusion,[19] we speculated that analogues of bicyclo-

[*] J. Dommerholt,[+] R. Temming, L. J. A. Hendriks, F. P. J. T. Rutjes, J. C. M. van Hest, F. L. van Delft
Radboud University Nijmegen
Institute for Molecules and Materials
Heijendaalseweg 135, 6525 AJ, Nijmegen (The Netherlands)
E-mail: f.vandelft@science.ru.nl
S. Schmidt,[+] P. Friedl
Radboud University Nijmegen
Nijmegen Center for Molecular Life Sciences
Department of Cell Biology, 6500 HB Nijmegen (The Netherlands)
D. J. Lefeber
Radboud University Medical Center
Department of Laboratory Medicine
6525 ED Nijmegen (The Netherlands)

[+] These authors contributed equally to this work.

[**] This research has been financially supported (in part) by the Council for Chemical Sciences of The Netherlands Organization for Scientific Research (NWO-CW, to F.L.D). Dr. G. J. Boons (Complex Carbohydrate Research Center, Athens, GA) is kindly acknowledged for fruitful discussions.

Supporting information for this article is available on the WWW under http://dx.doi.org/10.1002/anie.201003761.

[6.1.0]nonyne (compound **6**, Scheme 2a) would form a class of versatile cycloalkynes for bioconjugation by combining relative stability with high reactivity. Thus, the synthesis of BCN started by the dropwise addition of ethyl diazoacetate to a large excess (8 equiv) of 1,5-cyclooctadiene in the presence of rhodium acetate.[20] The resulting mixture of diastereomeric compounds *exo*-**5** and *endo*-**5**, formed in a 2:1 ratio, was readily separated by chromatography on silica gel (combined yield 76%). Next, as exemplified for *endo*-**5**, the individual stereoisomers were converted into the corresponding hydroxyalkynes by reduction of the ester group, bromination, and elimination—a three-step reaction sequence that was performed within eight hours and required only a single purification step. The desired bicyclo[6.1.0]non-4-yn-9-ol (*endo*-**6**) was thus obtained in 61% overall yield after purification (the diastereomeric *exo*-isomer of **6** was prepared in 53% yield form *exo*-**5**). Both *exo*-**6** or *endo*-**6** were found sufficiently stable for prolonged storage at −20 °C and did not undergo structural change upon stirring in the presence of 5 mM glutathione for 48 hours in CD_3CN/D_2O (1:2).[17]

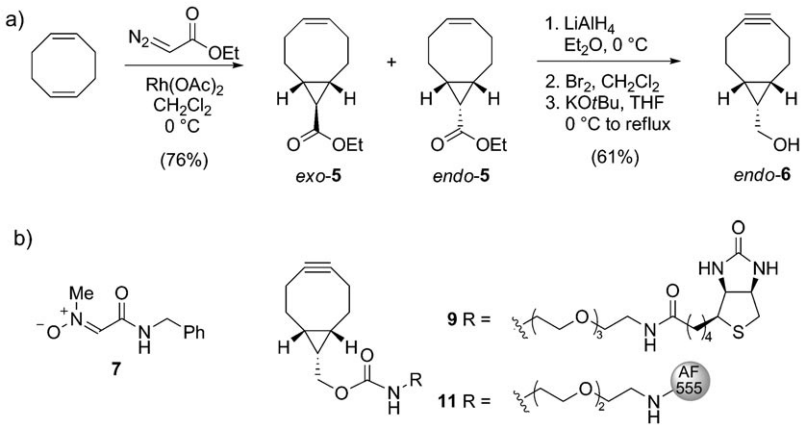

Scheme 2. a) Synthesis of 9-hydroxymethylbicyclo[6.1.0]nonyne (*endo*-**6**). b) Structures of nitrone **7** and BCN conjugated to biotin (**9**) or Alexa Fluor 555 (**11**). THF = tetrahydrofuran.

Next, we investigated the reaction kinetics of **6** in the prototypical SPAAC reaction with benzyl azide. Calculation of second-order reaction kinetics demonstrated that the three-membered ring fusion leads to a near 100-fold rate enhancement over plain cyclooctyne ($k \approx 2 \times 10^{-3}\,M^{-1}s^{-1}$), measuring $0.14\,M^{-1}s^{-1}$ for *endo*-**6** and $0.11\,M^{-1}s^{-1}$ for *exo*-**6**. Reaction rates increased, as anticipated,[13] in a more polar mixture (CD_3CN/D_2O (1:2)), measuring 0.29 and $0.19\,M^{-1}s^{-1}$ for *endo*-**6** and *exo*-**6**, respectively, values similar to or better than other cyclooctyne systems.[4,21] Strain-promoted acetylene–nitrone cycloaddition (SPANC)[13] with nitrone **7** (Scheme 2b) instead of an azide was found to be significantly faster, measuring 1.66 and $1.32\,M^{-1}s^{-1}$ for *endo*-**6** and *exo*-**6**, respectively.

The usefulness of BCN for bioorthogonal functionalization of biomolecules was next investigated in the one-pot SPANC functionalization of a model peptide with an N-terminal serine. Indeed, we observed a clean conversion of FRATtide, a GSK-1 binding peptide that prevents axin binding,[22] into the expected isoxazoline conjugates upon SPANC labeling with *endo*-**6** or biotinylated BCN-conjugate **9**, as judged by mass spectrometric analysis and spot-blot analysis (see the Supporting Information).

We also became interested in whether BCN-conjugates are suitable for labeling of azido-containing proteins. To this end, recombinant virus capsid protein was expressed in auxotrophic *E. coli* in the presence of azidohomoalanine,[23] thus leading to the introduction of a single azide in nearly 50% of the isolated protein. Without further separation, the mixture of proteins was subjected to strain-promoted functionalization with BCN-Alexa Fluor 555 conjugate **11** by mixing for three hours in a phosphate buffer (pH 7.5). After washing and dialysis, incorporation of **11** was confirmed by sodium dodecyl sulfate polyacrylamide gel electrophoresis (SDS-PAGE; Figure 1a) and mass spectrometric analysis, which indicated a quantitative mass increase of 1135 Da, that is, the molecular weight of **11** (see the Supporting Information). Next, capsid proteins were assembled into viral capsids by dialysis to a sodium acetate buffer (pH 5.0, 0.01M $CaCl_2$), and subsequently purified by FPLC. A strongly fluorescent peak appeared around 1.2 mL, which is the common elution volume of virus capsid. Finally, the structure of virus capsids was determined by transmission emission spectroscopy (TEM) indicating the structural integrity of the protein capsids after functionalization with **11** (Figure 1b).

The bioavailability and tolerability of labeling surface glycans on living human melanoma MV3 cells was addressed using the chemical reporter strategy.[1b] MV3 melanoma cells are highly invasive and metastatic, and their abundant production of surface glycans was previously implicated in invasion processes.[24] Thus, MV3 cells were incubated with

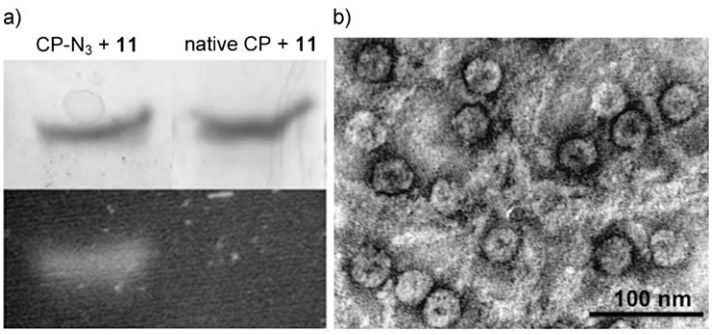

Figure 1. BCN modification of azido-containing virus capsid protein and assembly into virus capsids. a) SDS-PAGE analysis of reaction of BCN-AF555 conjugate (**11**) with capsid protein containing azide (left) or without azide (right). Top: Coomassie Brilliant Blue staining, bottom: fluorescence image. b) TEM pictures of fluorescent capsids (images recorded on a JEOL 1010 TEM, the sample was deposited on a hydrophilized Formvar carbon-coated TEM grid and consequently negatively stained with 0.2% uranyl acetate).

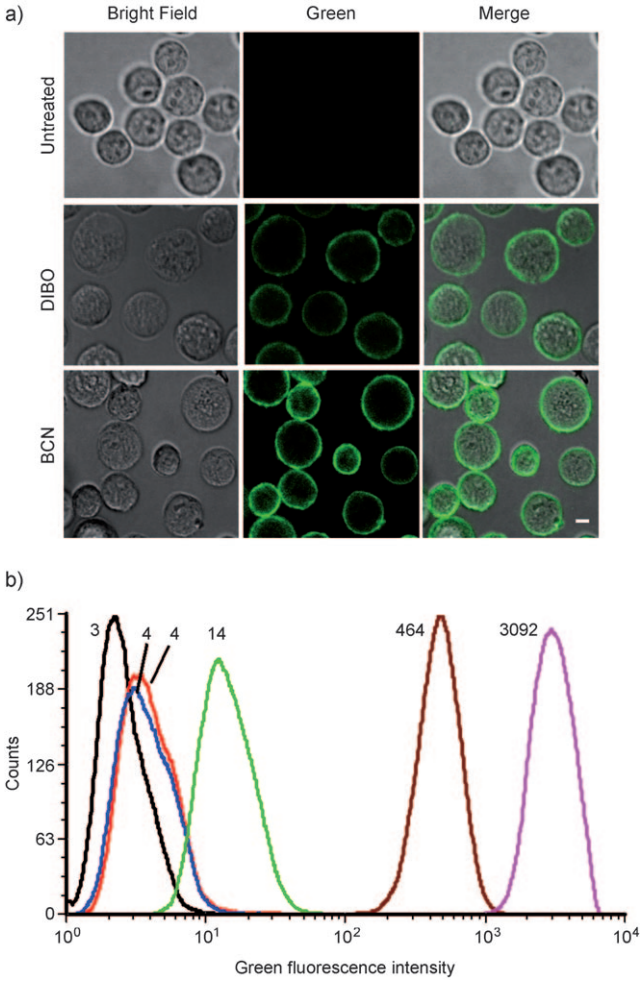

Figure 2. Surface and total fluorescence intensity of MV3 melanoma, cultured in the absence or presence of $Ac_4ManNAz$ (50 μM), followed by labeling with a cyclooctyne-biotin conjugate and secondary labeling with streptavidin-Alexa Fluor 488. a) Representative confocal images of unlabeled cells (top), cells labeled with DIBO-biotin (middle) or BCN-biotin **9** (bottom). Bar: 10 μm. b) Label intensity assessed by flow cytometry, indicated as mean fluorescence intensity (MFI). Numbers denote the average of green fluorescent cells for that particular experiment. Black trace: untreated; red trace: $Ac_4ManNAz$ + SA-AF488; blue trace: w/o $Ac_4ManNAz$ + DIBO + SA-AF488; dark red trace: $Ac_4ManNAz$ + DIBO + SA-AF488; green trace: w/o $Ac_4ManNAz$ + BCN + SA-AF488; magenta trace: $Ac_4ManNAz$ + BCN + SA-AF488.

peracetylated *N*-azidoacetyl-D-mannosamine ($Ac_4ManNAz$), labeled with BCN-biotin conjugate **9**, and stained with streptavidin-Alexa Fluor 488 (Figure 2). To be able to compare the efficiency of labeling of **9** to that of dibenzocyclooctyne (DIBO, **2**), one of the most reactive cyclooctyne systems known to date,[18] cells were also labeled with a DIBO-biotin conjugate. In all cases, cells retained morphological integrity and cell surface fluorescence, with consistently higher labeling for BCN than for DIBO, as detected by confocal microscopy (Figure 2a) and flow cytometry (Figure 2b). By using flow cytometry, high monophasic intensities and excellent signal-to-noise ratio (SNR) were found for both DIBO-biotin (SNR = 116) and BCN-biotin (SNR = 221). No signs of label-induced cytotoxicity were detected after propidium iodide staining (see the Supporting Information).

Functional cell integrity was confirmed after incorporating MV3 cells into three-dimensional collagen lattices yielding spontaneous and vigorous invasion. Owing to its high signal-to-noise ratio, labeling with BCN revealed fine, subcellular details, which can discriminate surface glycan distribution states on individual living cells as shown by densitometry experiments (see the Supporting Information). Whereas cells in suspension retain a near-homogeneous distribution of azidosialic acids on the cell surface (as in Figure 2), invading cells show the redistribution and accumulation of sialic acid at actin-rich contact sites with collagen fibers, consistent with their role in cell adhesion and migration (Figure 3).[25,26,27] Thereby, submicron resolution reveals fine surface distribution of sialic acids at leading edge filopodia, focal clusters at actin-rich contact sites to collagen fibers, and substantial glycan-rich deposits into the tissue matrix from the trailing edge (see the Supporting Information).

In conclusion, in view of the non-toxic labeling procedure, the tunable fluorescent properties by choice of dye and the high signal-to-noise ratio, BCN will be useful for addressing molecular glycan function studies in live-cell and other systems. A key advantage of BCN over earlier cyclooctynes lies in the combination of its exceptionally easy preparation with high reactivity. Furthermore, it should be noted that the lack of conformational isomerism in bicyclo[6.1.0]non-4-ynes[29] leads to sharp peaks in the ^1H NMR spectrum, which is further simplified by the C_s symmetry of BCN. An additional advantage of a symmetrical cyclooctyne is the formation of a single regioisomer upon cycloaddition, an aspect of particular advantage in areas where the formation of

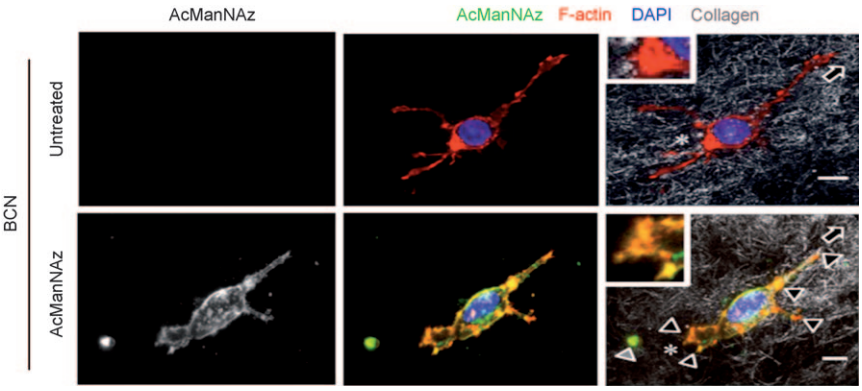

Figure 3. Live-cell staining and redistribution of glycans during invasive cell migration through a three-dimensional collagen matrix. Focal accumulation of sialic acid on migrating MV3 melanoma cell at interaction sites to collagen fibers and partial colocalization with F-actin. Insets, trailing edge. Direction of migration was determined from retraction fibers (asterisks) and deposited sialic acid-rich material lacking F-actin from the cell rear (gray arrowhead).[28] Bar: 5 μm. Focalized glycan distribution at cell matrix interactions (black arrowheads).

homogeneous adducts is mandatory.[11] Thus, BCN will allow a broad range of applications that require the highly efficient and metal-free conjugation of two separate molecular entities, for example in life sciences, material science, surface modification, and molecular diagnostics.

Received: June 19, 2010
Published online: ■■ ■■, 2010

Keywords: cycloadditions · cycloalkynes · imaging · kinetics · protein modification

[1] a) M. D. Best, *Biochemistry* **2009**, *48*, 6571 – 6584; b) E. M. Sletten, C. R. Bertozzi, *Angew. Chem.* **2009**, *121*, 7108 – 7133; *Angew. Chem. Int. Ed.* **2009**, *48*, 6974 – 6998.
[2] J. A. Prescher, C. R. Bertozzi, *Nat. Chem. Biol.* **2005**, *1*, 13 – 21.
[3] G. Charron, J. Wiljon, H. C. Hang, *Curr. Opin. Chem. Biol.* **2009**, *13*, 382 – 391.
[4] M. F. Debets, C. W. J. van der Doelen, F. P. J. T. Rutjes, F. L. van Delft, *ChemBioChem* **2010**, *11*, 1168 – 1184.
[5] M. Meldal, C. W. Tornøe, *Chem. Rev.* **2008**, *108*, 2952 – 3015.
[6] A. J. Link, M. K. S. Vink, D. A. Tirrell, *J. Am. Chem. Soc.* **2004**, *126*, 10598 – 10602.
[7] J. Gierlich, G. A. Burley, P. M. E. Gramlich, D. M. Hammond, T. Carell, *Org. Lett.* **2006**, *8*, 3639 – 3642.
[8] E. Lallana, E. Fernandez-Megia, R. Riguera, *J. Am. Chem. Soc.* **2009**, *131*, 5748 – 5750.
[9] C. R. Becer, R. Hoogenboom, U. Schubert, *Angew. Chem.* **2009**, *121*, 4998 – 5006; *Angew. Chem. Int. Ed.* **2009**, *48*, 4900 – 4908.
[10] M. Köhn, R. Breinbauer, *Angew. Chem.* **2004**, *116*, 3168 – 3178; *Angew. Chem. Int. Ed.* **2004**, *43*, 3106 – 3116.
[11] J.-F. Lutz, *Angew. Chem.* **2008**, *120*, 2212 – 2214; *Angew. Chem. Int. Ed.* **2008**, *47*, 2182 – 2184.
[12] a) A. T. Blomquist, L. H. Liu, *J. Am. Chem. Soc.* **1953**, *75*, 2153 – 2154; b) N. J. Agard, J. A. Prescher, C. R. Bertozzi, *J. Am. Chem. Soc.* **2004**, *126*, 15046 – 15047.
[13] X. Ning, R. P. Temming, J. Dommerholt, J. Guo, D. B. Ania, M. F. Debets, M. A. Wolfert, G. J. Boons, F. L. van Delft, *Angew. Chem.* **2010**, *122*, 3129 – 3132; *Angew. Chem. Int. Ed.* **2010**, *49*, 3065 – 3068.
[14] C. S. McKay, J. Moran, J. P. Pezacki, *Chem. Commun.* **2010**, *46*, 931 – 933.
[15] J. A. Codelli, J. M. Baskin, N. J. Agard, C. R. Bertozzi, *J. Am. Chem. Soc.* **2008**, *130*, 11486 – 11493.
[16] M. F. Debets, S. S. van Berkel, S. Schoffelen, F. P. J. T. Rutjes, J. C. M. van Hest, F. L. van Delft, *Chem. Commun.* **2010**, *46*, 97 – 99.
[17] J. C. Jewett, E. M. Sletten, C. R. Bertozzi, *J. Am. Chem. Soc.* **2010**, *132*, 3688 – 3690.
[18] X. Ning, J. Guo, M. A. Wolfert, G.-J. Boons, *Angew. Chem.* **2008**, *120*, 2285 – 2287; *Angew. Chem. Int. Ed.* **2008**, *47*, 2253 – 2255.
[19] H. Meier, C. Schuh-Popitz, H. Peiersen, *Angew. Chem.* **1981**, *93*, 286 – 287; *Angew. Chem. Int. Ed. Engl.* **1981**, *20*, 270 – 271.
[20] *Modern Rhodium-Catalyzed Organic Reactions* (Ed.: P. A. Evans), Wiley-VCH, Weinheim, **2005**.
[21] N. J. Agard, J. M. Baskin, J. A. Prescher, A. Lo, C. R. Bertozzi, *ACS Chem. Biol.* **2006**, *1*, 644 – 648.
[22] G. M. Thomas, S. Frame, M. Goedert, I. Nathke, P. Polakis, P. Cohen, *FEBS Lett.* **1999**, *458*, 247 – 251.
[23] A. J. Link, D. A. Tirrell, *Methods* **2005**, *36*, 291 – 298.
[24] M. Goebeler, D. Kaufmann, E. B. Brocker, C. E. Klein, *J. Cell Sci.* **1996**, *109*, 1957 – 1964.
[25] C. H. Chiang, C. H. Wang, H. C. Chang, S. V. More, W. S. Li, W. C. Hung, *J. Cell. Physiol.* **2010**, *223*, 492 – 499.
[26] D. R. Christie, F. M. Shaikh, J. A. Lucas IV, J. A. Lucas III, S. L. Bellis, *J. Ovarian Res.* **2008**, *1*, 3.
[27] E. C. Seales, G. A. Jurado, B. A. Brunson, J. K. Wakefield, A. R. Frost, S. L. Beilis, *Cancer Res.* **2005**, *65*, 4645 – 4652.
[28] C. Mayer, K. Maaser, N. Daryab, K. S. Zanker, E. B. Brocker, P. Friedl, *Eur. J. Cell Biol.* **2004**, *83*, 709 – 715.
[29] C. Antony-Mayer, H. Meier, *Chem. Ber.* **1988**, *121*, 2013 – 2018.

Communications

Bimolecular Imaging

J. Dommerholt, S. Schmidt, R. Temming, L. J. A. Hendriks, F. P. J. T. Rutjes, J. C. M. van Hest, D. J. Lefeber, P. Friedl, F. L. van Delft* _____ ■■■■–■■■■

Readily Accessible Bicyclononynes for Bioorthogonal Labeling and Three-Dimensional Imaging of Living Cells

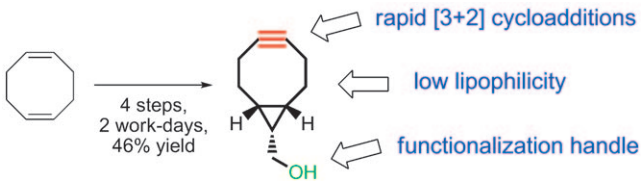

I can see clearly now: Bicyclo[6.1.0]non-4-yne, an easily prepared, symmetrical cycloalkyne, displays excellent reaction kinetics in strain-promoted cycloaddition reactions with azides and nitrones (see scheme). Highly specific protein modifications are demonstrated in vitro and subcellular-resolved imaging of glycan expression was achieved in metastatic melanoma cells during invasive migration into three-dimensional collagen lattices.

Angewandte Chemie
Eine Zeitschrift der Gesellschaft Deutscher Chemiker

Supporting Information

69451 Weinheim, Germany

Readily Accessible Bicyclononynes for Bioorthogonal Labeling and Three-Dimensional Imaging of Living Cells**

*Jan Dommerholt, Samuel Schmidt, Rinske Temming, Linda J. A. Hendriks, Floris P. J. T. Rutjes, Jan C. M. van Hest, Dirk J. Lefeber, Peter Friedl, and Floris L. van Delft**

anie_201003761_sm_miscellaneous_information.pdf

Supporting Information

	Page
Detailed synthetic preparation and structural analysis of compounds **5**-**11** and cycloadducts	2
Rate plots for cycloaddition of *endo*-**6** and *exo*-**6** with benzyl azide	7
Rate plots for cycloaddition of *endo*-**6** and *exo*-**6** with nitrone **7**	9
Mass spectrometric analysis of SPANC labeling of FRATtide with *endo*-**6** or biotin-conjugate **9**.	11
Spot-blot analysis of biotinylated FRATtide	13
MS analysis of fluorescence labeling of capsid protein with BCN-Alexa Fluor 555 conjugate **11**	14
FPLC trace of the reaction mixture after assembly of fluorescent capsids by dialysis	16
Flow cytometry of glycan labeling	17
Procedures for confocal microscopy and 3D imaging of glycan redistribution during invasive cell migrations	19
Pixel densitometry	20
Literature references	21

Detailed synthetic preparation and structural analysis of compounds 5-11 and cycloadducts.

General methods and procedures

^{1}H NMR spectra were recorded in $CDCl_3$ or CD_3CN/D_2O mixtures on Bruker DMX 300 or Varian Inova-400 spectrometers at 300 K. TMS (δ_H 0.00) or CD_3CN (δ_H 1.94) was used as the internal reference. ^{13}C NMR spectra were recorded in $CDCl_3$ at 75 MHz on a Bruker DMX 300 spectrometer, using the central resonance of $CDCl_3$ (δ_C 77.0) as the internal reference. Mass spectra were obtained on Applied Biosystems Voyager DE-Pro MALDI-TOF (no calibration) or JEOL AccuToF. Chemicals were purchased from Aldrich and used without further purification. CH_2Cl_2, acetonitrile, THF, Et_2O and toluene were obtained dry from a MBRAUN SPS-800 solvent purification system; and CH_3OH was distilled from magnesium and iodine. Aqueous solutions are saturated unless otherwise specified. All reactions were performed under anhydrous conditions under argon and monitored by TLC on Kieselgel 60 F254 (Merck). Detection was by examination under UV light (254 nm) and by charring with 10% sulfuric acid in methanol or with aqueous $KMnO_4$. Silica gel (Acros 0.035-0.070 mm) was used for chromatography.

(1*R*,8*S*,9*r*,*Z*)-Ethyl bicyclo[6.1.0]non-4-ene-9-carboxylate (*exo*-5), and (1*R*,8*S*,9*s*,*Z*)-ethyl bicyclo[6.1.0]non-4-ene-9-carboxylate (*endo*-5)

To a solution of 1,5-cyclooctadiene (19.6 mL, 160 mmol) and $Rh_2(OAc)_4$ (380 mg, 0.86 mmol) CH_2Cl_2 (10 mL) was added dropwise in 3 h a solution of ethyl diazoacetate (2.1 mL, 20 mmol) in CH_2Cl_2 (10 mL). This solution was stirred for 40 h at rt. CH_2Cl_2 was evaporated and the excess of cyclooctadieen was removed by filtration over a glass filter filled with silica and elution with EtOAc:heptane, 1:200 (400 mL). The filtrate was concentrated *in vacuo* and the residue was purified by column chromatography on silica gel (EtOAc:heptane, 1:20) to afford *exo*-**5** (1.10 g, 28%) and *endo*-**5** (2.24 g, 58%) as colorless oils. R_F *exo*-**5** 0.24, R_F *endo*-**5** 0.33 (EtOAc:heptane, 1:20).

exo-**5**: ^{1}H NMR ($CDCl_3$, 400 MHz): δ 5.68-5.60 (m, 2H), 4.10 (q, J = 7.2 Hz, 2H), 2.35-2.27 (m, 2H), 2.24-2.16 (m, 2H), 2.13-2.04 (m, 2H), 1.59-1.53 (m, 2H), 1.53-1.43 (m, 2H), 1.25 (t, J = 7.2 Hz, 3H), 1.18 (t, J = 4.8 Hz, 1H). ^{13}C NMR ($CDCl_3$, 75 MHz): δ 174.3, 129.8, 60.1, 28.2, 27.8, 27.6, 26.6, 14.2. HRMS (FAB+) *m/z* calcd for $C_{12}H_{19}O_2$ $(M + H)^+$: 195.1385, found: 195.1388.

endo-**5**: ^{1}H NMR ($CDCl_3$, 400 MHz): δ 5.65-5.57 (m, 2H), 4.12 (q, J = 7.2 Hz, 2H), 2.53-2.46 (m, 2H), 2.25-2.16 (m, 2H), 2.10-2.01 (m, 2H), 1.87-1.79 (m, 2H), 1.70 (t, J = 8.8 Hz, 1H), 1.43-1.34 (m, 2H), 1.26 (t, J = 7.2 Hz, 3H). ^{13}C NMR ($CDCl_3$, 75 MHz): δ 172.2, 129.4, 59.7, 27.0, 24.1, 22.6, 21.2, 14.4. HRMS (FAB+) *m/z* calcd for $C_{12}H_{19}O_2$ $(M + H)^+$: 195.1385, found: 195.1378.

(1*R*,8*S*,9*s*)-Bicyclo[6.1.0]non-4-yn-9-ylmethanol (*endo*-6)

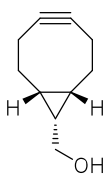

To a suspension of $LiAlH_4$ (90 mg, 2.34 mmol) in Et_2O (10 mL) was added dropwise at 0 °C a solution of *endo*-**5** (520 mg, 2.68 mmol) in Et_2O (10 mL). This suspension was

stirred for 15 min at rt, then cooled down to 0 °C, and water was added carefully until the grey solid had turned into white. Na_2SO_4 (2 g) was added, the solid was filtered off and washed thoroughly with Et_2O (100 mL). The filtrate was concentrated *in vacuo*.

Without further purification the alcohol was dissolved in CH_2Cl_2 (20 mL). At 0 °C a solution of Br_2 (151 µL, 2.94 mmol) in CH_2Cl_2 (2 mL) was added dropwise until the yellow color persisted. The reaction mixture was quenched with a 10% $Na_2S_2O_3$-solution (5 mL), and extracted with CH_2Cl_2 (2 x 20 mL). The organic layer was dried (Na_2SO_4) and concentrated *in vacuo* to afford the dibromide (833 mg, quant.).

Without further purification the dibromide (700 mg, 2.24 mmol) was dissolved in THF (25 mL). A solution of KO*t*Bu (7.4 mL, 1 M in THF, 7.40 mmol) was added dropwise at 0 °C. Then the solution was refluxed for 2 h. After cooling down to rt the mixture was quenched with saturated NH_4Cl-solution (20 mL), and extracted with CH_2Cl_2 (3 x 20 mL). The organic layer was dried (Na_2SO_4) and concentrated *in vacuo*. The residue was purified by column chromatography on silica gel (EtOAc:pentane, 1:1) to afford *endo*-**6** (205 mg, 61%) as a white solid. R_F 0.22 (EtOAc:pentane, 1:1).

^{1}H NMR ($CDCl_3$, 400 MHz): δ 3.73 (d, J = 8.0 Hz, 2H), 2.35-2.20 (m, 6H), 1.66-1.56 (m, 2H), 1.39-1.30 (m, 1H), 1.18 (bs, 1H), 0.99-0.90 (m, 2H). ^{13}C NMR ($CDCl_3$, 75 MHz): δ 98.4, 59.3, 28.5, 21.0, 20.9, 19.5.

(1*R*,8*S*,9*r*)-Bicyclo[6.1.0]non-4-yn-9-ylmethanol (*exo*-6)

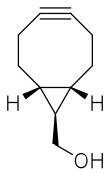

Compound *exo*-**6** was prepared by an identical procedure as described for *endo*-**6**. Final purification by column chromatography on silica gel (EtOAc:pentane, 1:1) afforded *exo*-**6** (128 mg, 53%) as a white solid. R_F 0.23 (EtOAc:pentane, 1:1).

^{1}H NMR ($CDCl_3$, 400 MHz): δ 3.54 (d, J = 6.4 Hz, 2H), 2.44-2.40 (m, 2H), 2.32-2.25 (m, 2H), 2.18-2.14 (m, 2H), 1.88 (bs, 1H), 1.44-1.34 (m, 2H), 0.74-0.63 (m, 3H). ^{13}C NMR ($CDCl_3$, 75 MHz): d 98.7, 66.9, 33.3, 27.2, 22.5, 21.4.

(1*R*,8*S*,9*s*)-Bicyclo[6.1.0]non-4-yn-9-ylmethyl (4-nitrophenyl) carbonate (8)

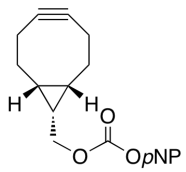

To a solution of *endo*-**6** (32 mg, 0.213 mmol) in CH_2Cl_2 (5 mL) was added pyridine (43 µL, 0.532 mmol) and *p*-NO_2PhOC(O)Cl (53 mg, 0.266 mmol). After stirring for 15 min at rt the mixture was quenched with saturated NH_4Cl-solution (5 mL) and extracted with CH_2Cl_2 (3 x 5 mL). The organic layer was dried (Na_2SO_4) and concentrated *in vacuo*. The residue was purified by column chromatography on silica gel (EtOAc:pentane, 1:5) to afford **8** (52 mg, 77%) as a white solid. R_F 0.30 (EtOAc:pentane, 1:3).

^{1}H NMR ($CDCl_3$, 400 MHz): δ 8.28 (d, J = 9.2 Hz, 2H), 7.40 (J = 9.6 Hz, 2H), 4.41 (d, J = 8.4 Hz, 2H), 2.37-2.22 (m, 6H), 1.67-1.57 (m, 2H), 1.56-1.47 (m, 1H), 1.11-1.02 (m, 2H). ^{13}C NMR ($CDCl_3$, 75 MHz): δ 155.6, 152.5, 145.3, 125.3, 121.7, 98.7, 68.0, 29.0, 21.3, 20.5, 17.2.

(1*R*,8*S*,9*S*)-bicyclo[6.1.0]non-4-yn-9-ylmethyl 12-(+)-biotinylamino-3,6,9-trioxa-dodecyl carbamate (9)

To a solution of **7** (52 mg, 0.165 mmol) in DMF (5 mL) was added (+)-biotin-$(PEO)_4$-NH_2 (69 mg, 0.165 mmol) and NEt_3 (69 µL, 0.495 mmol). After stirring for 2 h at rt the reaction mixture was evaporated to dryness *in vacuo*. The residue was purified by column chromatography on silica gel (acetone:MeOH, 9:1) to afford **9** (68 mg, 69%) as a white solid. R_F 0.22 (acetone:MeOH, 9:1).

^{1}H NMR ($CDCl_3$, 400 MHz): δ 6.76-6.69 (m, 1H), 6.61 (bs, 1H), 5.67 (bs, 1H), 5.40-4.34 (m, 1H), 4.52-4.49 (m, 1H), 4.33-4.30 (m, 1H), 4.15 (d, J = 8 Hz, 2H), 3.64-3.63 (m, 8H), 3.59-3.54 (m, 4H), 3.46-3.42 (m, 2H), 3.39-3.35 (m, 2H), 3.17-3.12 (m, 1H), 2.90 (dd, J = 12.8, 4.8 Hz, 1H), 2.75 (d, J = 12.8 Hz, 1H), 2.30-2.21 (m, 8H), 1.80-1.53 (m, 6H), 1.48-1.31 (m, 3H), 0.97-0.92 (m, 2H). HRMS (ESI+) *m/z* calcd for $C_{29}H_{47}N_4O_7S$ $(M + H)^+$: 595.3165, found: 595.3166.

(1*R*,8*S*,9*s*)-bicyclo[6.1.0]non-4-yn-9-ylmethyl 3,6,9-trioxa-12-azadodecylcarbamate (10)

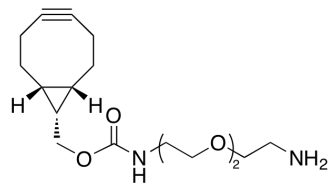

To a solution of **8** (14 mg, 0.044 mmol) in DMF (1 mL) was added 1,8-diamino-3,6-dioxaoctane (38 µL, 0.266 mmol) and NEt_3 (19 µL, 0.133 mmol) and the reaction mixture was stirred at rt for 15 min. The mixture was concentrated under reduced pressure, taken up in CH_2Cl_2 (20 mL) and extracted with 1 N NaOH (2 x 2 mL), followed by water (2 mL). The combined aqueous phases were extracted once with CH_2Cl_2 (10 mL) and extracted with water (2 mL). The combined organic layers were dried over Na_2SO_4 and concentrated *in vacuo*. Silica gel column chromatography (CH_2Cl_2:MeOH, 20:1 → 10:1 → 5:1, 1% Et_3N) and concentration *in vacuo* gave the title compound **10** (12 mg, 83%) as a slightly yellow oil. ^{1}H NMR ($CDCl_3$, 400 MHz): δ 5.34 (bs, 1H), 4.15 (d, 2H, J = 8.0 Hz), 3.62 (s, 4H), 3.58-3.48 (m, 4H), 3.38 (m, 2H), 2.89 (t, 3H, J = 5.2 Hz), 2.32-2.19 (m, 6H), 1.64-1.51 (m, 2H), 1.40-1.31 (m, 1H), 0.96-0.88 (m, 2H). ^{13}C NMR ($CDCl_3$, 75 MHz): δ 98.8, 73.4, 70.3, 70.2, 70.1, 62.7, 41.7, 40.8, 29.1, 21.4, 20.1, 17.8. HRMS (ESI+) *m/z* calcd for $C_{17}H_{28}N_2O_4$ $(M + H)^+$: 325.2122, found: 325.2120.

BCN-Alexa Fluor 555 conjugate (11)

To a solution of **10** (0.27 mg, 0.833 µmol) in DMF (1 mL) was added Alexa Fluor 555 carboxylic acid, succinimidyl ester (1 mg, 0.833 µmol). The reaction mixture was stirred for 16 h at rt, and any remaining unreacted Alexa Fluor 555 was quenched with ethanolamine (1 µL, 17 µmol) for 1 h at rt. The reaction mixture was then concentrated *in vacuo*. The crude product was used without any further purification.

((5a*R*,6*S*,6a*S*)-1-benzyl-1,4,5,5a,6,6a,7,8-octahydrocyclopropa[5,6]cycloocta[1,2-*d*][1,2,3]triazol-6-yl)methanol

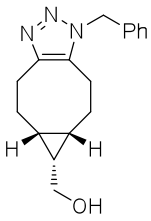

To a solution of *endo*-**6** (24 mg, 0.16 mmol) in a mixture of CH_3CN/H_2O=3/1 (7 mL) was added BnN_3 (19.9 µL, 0.16 mmol). This mixture was stirred for 16 h at rt, and then extracted with CH_2Cl_2 (3 x 5 mL). The organic layer was dried (Na_2SO_4) and concentrated *in vacuo*. The residue was purified by column chromatography on silica

gel (EtOAc) to afford the *endo*-cycloadduct (44 mg, 97%) as a white solid. R_F 0.11 (EtOAc). ^{1}H NMR ($CDCl_3$, 400 MHz): δ 7.34-7.26 (m, 3H), 7.11-7.09 (m, 2H), 5.52-5.42 (m, 2H), 3.68 (ddd, *J* = 25.7, 11.3, 7.8 Hz, 2H), 3.11 (ddd, *J* = 15.8, 7.3, 3.8 Hz, 1H), 2.91 (ddd, *J* = 15.8, 9.6, 4.0 Hz, 1H), 2.78 (ddd, *J* = 16.1, 6.6, 3.5 Hz, 1H), 2.55 (ddd, *J* = 16.1, 10.3, 3.7 Hz, 1H), 2.25-2.17 (m, 1H), 2.04-1.97 (m, 2H), 1.59-1.41 (m, 2H), 1.19-1.10 (m, 1H), 1.03-0.95 (m, 1H), 0.86-0.78 (m, 1H). ^{13}C NMR ($CDCl_3$, 75 MHz): δ 145.1, 135.2, 133.1, 128.8, 128.0, 126.8, 59.5, 51.9, 26.0, 23.1, 22.2, 21.5, 20.9, 19.3, 19.0. HRMS (ESI+) *m/z* calcd for $C_{17}H_{22}N_3O$ $(M + H)^+$: 284.1763, found: 284.1749.

((5a*R*,6*R*,6a*S*)-1-benzyl-1,4,5,5a,6,6a,7,8-octahydrocyclopropa[5,6]cycloocta[1,2-*d*][1,2,3]triazol-6-yl)methanol

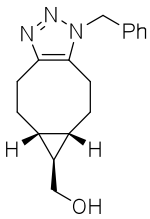

The *exo*-product was prepared by the same procedure as described for the *endo*-cycloadduct. The residue was purified by column chromatography on silica gel (EtOAc) to afford *exo*-cycloadduct (43 mg, 95%) as a white solid. R_F 0.10 (EtOAc). ^{1}H NMR ($CDCl_3$, 400 MHz): δ 7.33-7.28 (m, 3H), 7.11-7.09 (m, 2H), 5.46 (s, 2H), 3.50-3.40 (m, 2H), 3.09 (ddd, *J* = 15.9, 7.3, 3.3 Hz, 1H), 2.85 (ddd, *J* = 15.9, 10.1, 3.5 Hz, 1H), 2.73 (ddd, *J* = 16.2, 6.7, 3.0 Hz, 1H), 2.51 (ddd, *J* = 16.1, 10.5, 3.2 Hz, 1H), 2.41-2.33 (m, 1H), 2.22-2.15 (m, 2H), 1.39-1.30 (m, 1H), 1.27-1.18 (m, 1H), 0.83-0.76 (m, 1H), 0.70-0.62 (m, 2H). ^{13}C NMR ($CDCl_3$, 75 MHz): δ 145.4, 135.2, 133.3, 128.8, 128.0, 126.8, 66.1, 51.9, 27.6, 27.1, 26.3, 25.8, 22.9, 22.0, 21.9. HRMS (ESI+) *m/z* calcd for $C_{17}H_{22}N_3O$ $(M + H)^+$: 284.1763, found: 284.1746.

(5a*S*,6*S*,6a*R*)-*N*-benzyl-6-(hydroxymethyl)-2-methyl-3,4,5,5a,6,6a,7,8-octahydro-2*H*-cyclopropa[5,6]cycloocta[1,2-*d*]isoxazole-3-carboxamide

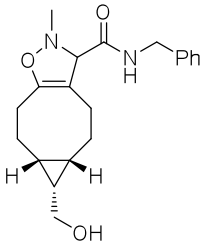

To a solution of *endo*-**6** (54 mg, 0.36 mmol) in a mixture of CH_3CN/H_2O=3/1 (7 mL) was added nitrone **7** (70 mg, 0.36 mmol). This mixture was stirred for 16 h at rt, and then extracted with CH_2Cl_2 (3 x 5 mL). The organic layer was dried (Na_2SO_4) and concentrated *in vacuo*. The residue was purified by column chromatography on silica gel (EtOAc:heptane, 2:1) to afford *endo*-cycloadduct as a mixture of isomers (114 mg, 92%). R_F 0.17 (EtOAc:heptane, 4:1). ^{1}H NMR ($CDCl_3$, 400 MHz): δ 7.58-7.52 (m, 1H), 7.34-7.22 (m, 5H), 4.52-4.46 (m, 1H), 4.41-4.34 (m, 1H), 3.93 (s, 0.4H), 3.88 (s, 0.6H), 3.74-3.65 (m, 2H), 2.81-2.73 (m, 1H), 2.69 (2s, 3H), 2.43-2.19 (m, 3H), 2.08-1.94 (m, 3H), 1.65-1.44 (m, 2H), 1.19-1.06 (m, 1H), 1.03-0.95 (m, 1H), 0.90-0.83 (m, 1H). ^{13}C NMR ($CDCl_3$, 75 MHz): δ 170.4, 146.3, 146.1, 138.3, 138.2, 128.7, 128.5, 127.5, 127.3, 103.1, 102.8, 79.8, 79.3, 59.7, 46.1, 42.8, 39.1, 25.9, 25.5, 25.2, 21.6, 20.6, 20.5, 19.8, 19.6, 19.2, 18.6, 18.3, 18.1. HRMS (ESI+) *m/z* calcd for $C_{20}H_{27}N_2O_3$ $(M + H)^+$: 343.2022, found: 343.2008.

(5a*S*,6*R*,6a*R*)-*N*-benzyl-6-(hydroxymethyl)-2-methyl-3,4,5,5a,6,6a,7,8-octahydro-2*H*-cyclopropa[5,6]cycloocta[1,2-*d*]isoxazole-3-carboxamide

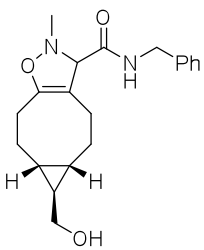

The *exo*-product was prepared by the same procedure as described for *endo*-cycloadduct. The residue was purified by column chromatography on silica gel

(EtOAc:CH_2Cl_2, 5:1) to afford the *exo*-cycloadduct as a mixture of isomers (28 mg, 88%). R_F 0.11 (EtOAc:heptane, 2:1).

^{1}H NMR ($CDCl_3$, 400 MHz): δ 7.55-7.49 (m, 1H), 7.34-7.24 (m, 5H), 4.52-4.33 (m, 2H), 3.91 (s, 0.5H), 3.87 (s, 0.5H), 3.54-3.40 (m, 2H), 2.78-2.72 (m, 0.5H), 2.69 (2s, 3H), 2.61-2.53 (m, 0.5H), 2.40-2.31 (m, 1H), 2.28-2.11 (m, 4H), 1.50-1.26 (m, 3H), 0.79-0.62 (m, 3H). ^{13}C NMR ($CDCl_3$, 75 MHz): δ 170.4, 170.3, 146.3, 138.4, 138.3, 128.6, 128.5, 127.6, 127.4, 127.3, 103.3, 103.0, 80.0, 79.6, 66.6, 46.2, 42.9, 42.7, 26.7, 26.6, 26.4, 25.9, 25.7, 25.4, 25.1, 24.3, 24.2, 21.4, 21.2, 20.9, 20.8. HRMS (ESI+) *m/z* calcd for $C_{20}H_{27}N_2O_3$ $(M + H)^+$: 343.2022, found: 343.2010.

Rate plots for cycloaddition of *endo*-6 and *exo*-6 with benzyl azide

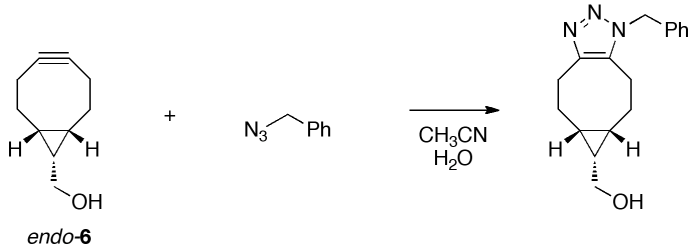

endo-**6**

same for *exo*-**6**

	$CD_3CN:D_2O=3:1$	$CD_3CN:D_2O=1:2$
endo-**6**	**A** 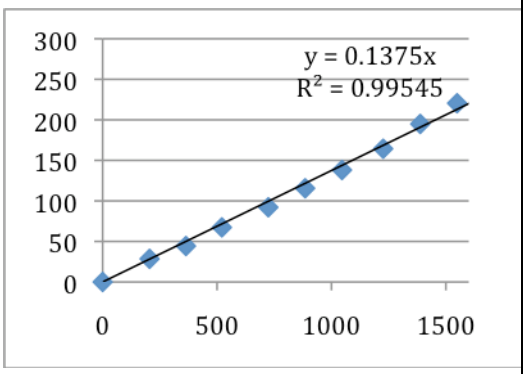	**B** 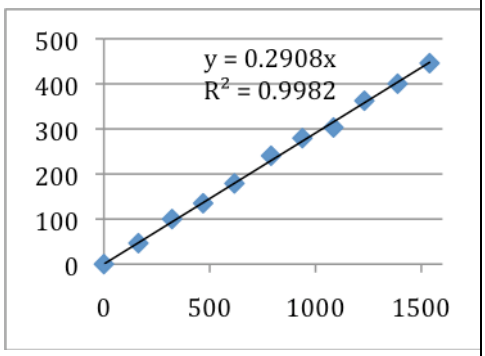
exo-**6**	**C** 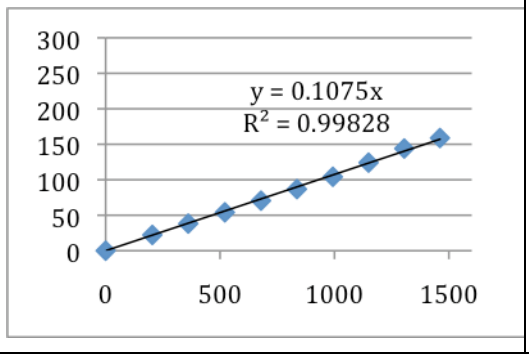	**D** 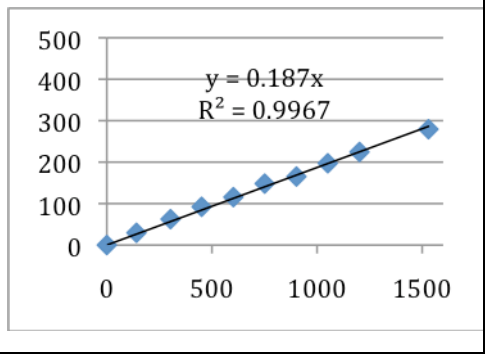

All experiments were conducted at 18 mM concentration.

^{1}H-NMR monitoring of cycloaddition of *exo*-**6** or *endo*-**6** with benzyl azide was performed by rapid mixing (t=0) of stock solutions A and B (0.3 mL each) in an NMR tube and immediate insertion into a 400 MHz NMR spectrometer. NMR spectra were measured at preset time-intervals. Each experiment was performed in triplo.

Stock solution A: alkyne **6** was dissolved in a mixture of CD_3CN and D_2O (ratio 3:1 or 1:2, 10 mL) to give a 36 mM solution.

Stock solution B: benzyl azide was dissolved in a mixture of CD_3CN and D_2O (ratio 3:1 or 1:2, 10 mL) to give a 32.8 mM solution.

Kinetics of the reaction of *exo*-**6** or *endo*-**6** with benzyl azide were determined by measuring the decrease of the integral of the signal caused by benzyl azide methylene protons, with the integral of the acetonitrile or water solvent-peak as internal standard. A starting value for the integral of the methyl signals was estimated, due to the fact that cycloaddition had already proceeded significantly by the time of the first measurement. From the conversion plots thus obtained, the second order rate plots were calculated according to equation:

$$kt = \frac{1}{[B]_0 - [A]_0} \times \ln \frac{[A]_0([B]_0 - [P])}{([A]_0 - [P])[B]_0} \qquad (1)$$

with k = 2nd order rate constant ($M^{-1}s^{-1}$), t = reaction time (s), $[A]_0$ = the initial concentration of substrate A (mmol/mL), $[B]_0$ = the initial concentration of substrate B (mmol/mL) and $[P]$ = the concentration of product (mmol/mL).

Rate plots for cycloaddition of *endo*-6 and *exo*-6 with nitrone 7

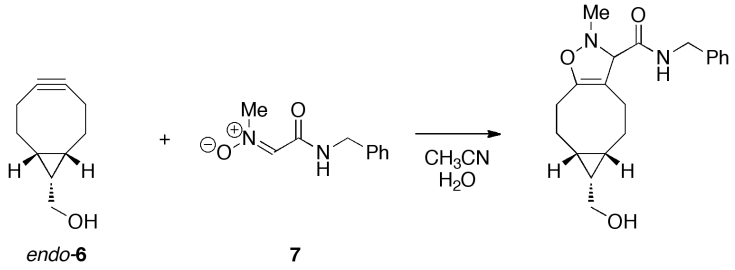

endo-**6** **7**

same for *exo*-**6**

endo-**6**	**A** 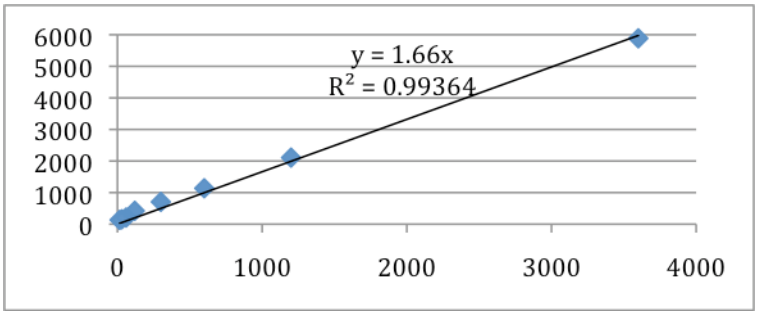
exo-**6**	**B** 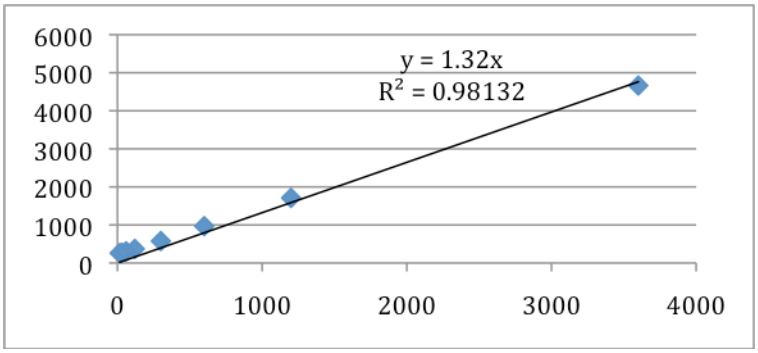

All experiments were conducted at 18 mM concentration in CD_3CN:D_2O=3:1.

^{1}H-NMR monitoring of cycloaddition of *exo*-**6** or *endo*-**6** with nitrone **7** was performed by rapid mixing (t=0) of stock solutions A and B (0.3 mL each) in an NMR tube and immediate insertion into a 400 MHz NMR spectrometer. NMR spectra were measured at preset time-intervals. Each experiment was performed in triplo.

Stock solution A: alkyne **6** was dissolved in a mixture of CD_3CN and D_2O (ratio 3:1 or 1:2, 10 mL) to give a 36 mM solution.

Stock solution B: *N*-(methyliminoacetyl *N*-oxide)benzylamine (nitrone **7**) was dissolved in a mixture of CD_3CN and D_2O (ratio 3:1 or 1:2, 10 mL) to give a 32.8 mM solution.

Kinetics of the reaction of *exo*-**6** or *endo*-**6** with nitrone **7** were determined by measuring the decrease of the integral of the nitrone methyl groups, with the integral of the acetonitrile or water solvent peak as internal

standard. A starting value for the integral of the methyl signals was estimated, due to the fact that cycloaddition had already proceeded significantly by the time of the first measurement.

From the conversion plots thus obtained, the second order rate plots were calculated according to equation:

$$kt = \frac{1}{[B]_0 - [A]_0} \times \ln \frac{[A]_0([B]_0 - [P])}{([A]_0 - [P])[B]_0} \quad (1)$$

with k = 2nd order rate constant ($M^{-1}s^{-1}$), t = reaction time (s), $[A]_0$ = the initial concentration of substrate A (mmol/mL), $[B]_0$ = the initial concentration of substrate B (mmol/mL) and $[P]$ = the concentration of product (mmol/mL).

Mass spectrometric analysis of SPANC labeling of FRATtide with *endo*-6 and biotin-conjugate 9.

a)

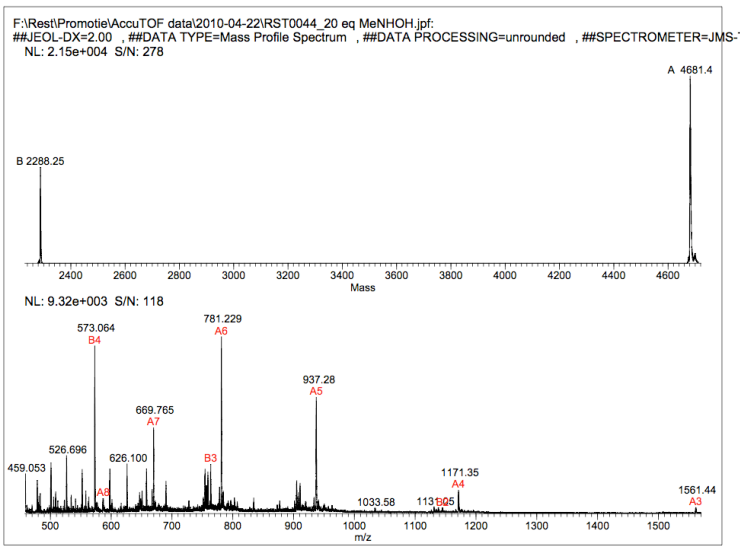

b)

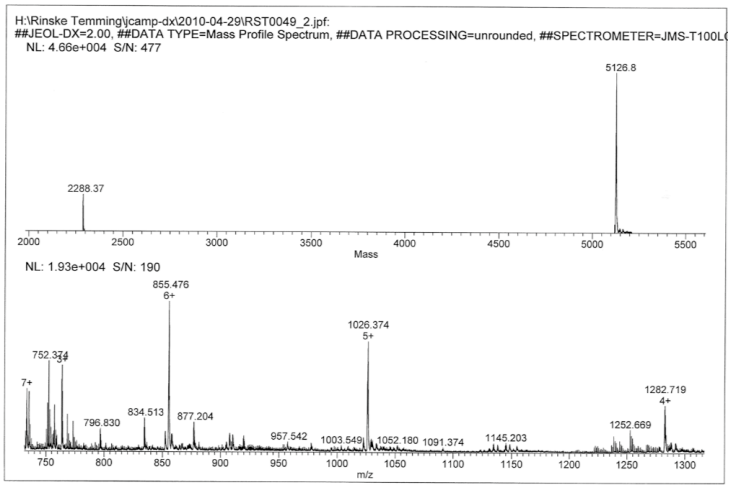

SPANC labeling of FRATtide with *endo*-6 (top)

FRATtide (15.6 µg, 3.4 nmol, 34 µM) was dissolved in 0.1 M NH_4OAc buffer pH 6.9 (100 µL) and $NaIO_4$ (1.1µg, 5.5 nmol, 48 µM) was added. The reaction was allowed to take place at room temperature for 40 min and p-methoxybenzenethiol (9.2 µg, 66.0 nmol, 565 µM) was added. The mixture was shaken for 2h at 25 °C and *p*-anisidine (13.5 µg, 109.3 nmol, 845 µM), *N*-methylhydroxylamine hydrochloride (18.2 µg, 218.6 nmol, 1.5 mM), and *endo*-**6** (41.1 µg, 273.3 nmol, 1.8 mM) were added. Finally, the reaction mixture was shaken at 25 °C for 24 h to give the desired conjugate. MS (Accu-TOF) measurement gave 4681.4 Da as the main peak after deconvolution.

SPANC labeling of FRATtide with BCN-biotin conjugate 9 (bottom)

FRATtide (9.3 µg, 2.1 nmol, 35 µM) was dissolved in 0.1 M NH_4OAc buffer pH 6.9 (60 µL) and $NaIO_4$ (0.7µg, 3.4 nmol, 52 µM) was added. The reaction was allowed to take place at room temperature for 40 min and *p*-methoxybenzenethiol (5.7 µg, 40.7 nmol, 581 µM) was added. The mixture was shaken for 2 h at 25 °C and *p*-anisidine (8.3 µg, 67.2 nmol, 864 µM), *N*-methylhydroxylamine hydrochloride (11.3 µg, 134.8

nmol, 1.6 mM), and **9** (100.3 µg, 168.6 nmol, 1.7 mM) were added. Finally, the reaction mixture was shaken at 25 °C for 24 h to give the desired conjugate. The residue was purified using an YM-3 millipore microcon centrifugal filter device by centrifuging three times for 30 min at 13,000 x g with 300 µL 0.1 M NH_4OAc buffer pH 6.9. MS (Accu-TOF) measurement gave 5126.8 Da as the main peak after deconvolution.

Spot-blot analysis of biotinylated FRATtide

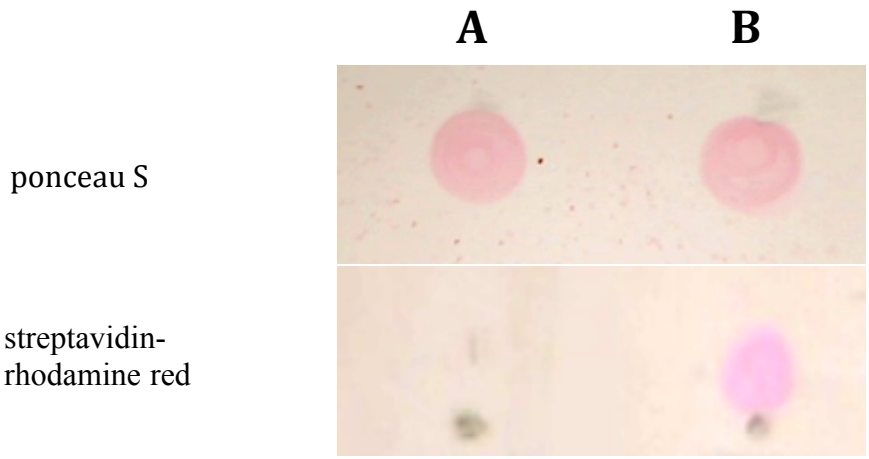

1 µL of native FRATtide (A) or purified FRATtide-BCN-biotin conjugate (B) were spotted on Whatman nitrocellulose membrane. Non-specific sites were blocked using 5% BSA in TBS-T (20 min). Top: proteins were stained using ponceau S. Bottom: proteins were stained with TBS-T solution containing 1% BSA and 0.01% rhodamine red-labeled streptavidin (Invitrogen) for 5 min.

After absorption of the peptide to the membrane, it can be reversibly stained with ponceau S, which stains all peptides and proteins present, showing that there are equal amounts of protein in each spot. Incubation with labeled streptavidin, followed by washing, shows that only the FRATtide-BCN-biotin conjugate (B) binds to the streptavidin, but there is no staining for FRATtide alone (A). This indicates that the conjugation of biotin to the FRATtide was successful and that there is no aspecific absorption taking place at non-functionalized FRATtide.

MS analysis of fluorescence labeling of capsid protein with BCN-Alexa Fluor 555 conjugate 11.

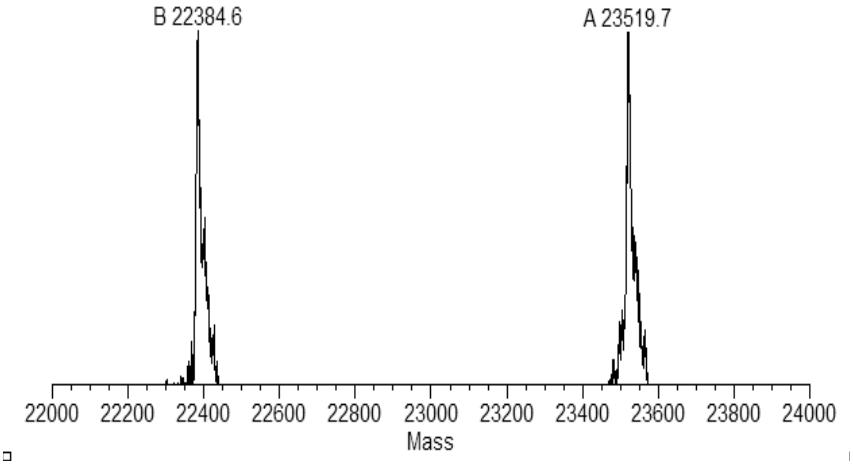

ESI-TOF mass spectrum of capsid protein reacted with **10**. Peak B corresponds to the mass of unreacted CP, while peak A corresponds to the reaction product. The mass difference between the peaks is 1135.1 (expected 1135).

The capsid protein (CP) of Cowpea Chlorotic Mottle Virus (CCMV) was expressed recombinantly in methionine auxotroph *E. coli*. The gene encoding the CP was obtained as described by Minten *et al.*[1] The wild-type CP contains two methionines, Met1 and Met137, and due to the cloning procedure a third methionine was added at the N-terminus of the protein. Site-directed mutagenesis was used to mutate two of these methionines into alanines. First Met137→Ala was mutated with the primer set CGAAAGATGTTGTCGCTGCTGCGTACCCCGAGGCG (mutation site underlined) and its reverse complement using the following PCR program: [95 °C, 1'; 16 cycles of (95 °C, 30"; 55 °C, 1'; 68 °C, 15'); 68 °C, 5']. Consequently Met1→Ala was mutated using the primer-set CGCGGCAGCCATATGGCGTCTACAGTCGGAACAG (mutation site underlined) and its reverse complement using the same PCR program. Both mutations were confirmed by sequence analysis.

Recombinant expression

For recombinant expression, the plasmid containing the CP-gene was transformed to a strain of methionine-auxotroph *E.coli* bacteria (B834 (DE3) pLysS cells, Novagen). The auxotroph expression was performed following the general procedure described by Link *et al.*[2] with some modifications. The bacteria were cultured in LB medium supplemented with ampicillin (100 mg/L) and chloramphenicol (50 mg/L) until an optical density of 0.4 - 0.6 was reached, at which point IPTG (final concentration 1 mM) was added to allow synthesis of T7 polymerase in presence of methionine. After 15 minutes the culture was washed twice by centrifugation and resuspension in 0.9% NaCl, followed by resuspension in M9 minimal medium supplemented with all natural amino acids (40 mg/L each) except methionine, glucose (0.4%), $MgSO_4$ (1 mM), thiamine (0.0005%), ampicillin (100 mg/L) and chloramphenicol (50 mg/L). The bacteria were cultured at 37 °C for 15 minutes before azidohomoalanine (40 mg/L) and IPTG (1 mM) were added to start the production of azido-containing CP. After culturing the bacteria for 18 hours at 30 °C the bacteria were harvested by centrifugation.

The CP was purified by Ni^{2+} NTA affinity chromatography under native conditions (Qiagen, Hilden, Germany). After purification the protein was analyzed by SDS-PAGE and mass spectroscopy, the latter indicating that approximately 50% of the proteins contains an azidohomoalanine instead of a methionine (data not shown). The N-terminal location of this this azide group ensures its positioning on the inside surface of the virus capsid after assembly from the capsid proteins.

Protein functionalization

The mixture of singly functionalized proteins and non-functionalized proteins (1 mg/ml in 0.1M phosphate buffer pH 7.5, 1M NaCl) was mixed with 4 equivalents of Alexa Fluor-BCN conjugate 11, which was dissolved in a minute amount of water. After mixing for 3 hours at RT, the reaction product was analyzed on a 12% SDS PAGE gel, of which a fluorescence image was obtained before staining it with Coomassie Blue stain. As control reaction Alexa Fluor-BCN conjugate 11 was mixed with non-functionalized CP protein in exactly the same conditions as the reaction. The absence of fluorescence in the fluorescence image shows that there is neither a side reaction nor any non-covalent adhesion of the dye to the protein.

To obtain a mass spectrum of the reaction product, the product was dialyzed to 0.1% formic acid in water (using Microcon® centrifugal filter units, 10 kDa, Millipore) before injecting it into the ESI-TOF (JEOL AccuTOF) mass spectrometer. Deconvolution of the raw data resulted in the spectrum displayed in Figure 5.

FPLC trace of the reaction mixture after assembly of fluorescent capsids by dialysis

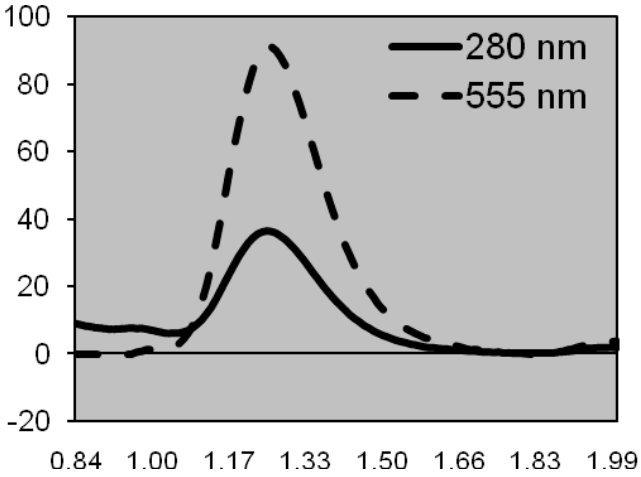

FPLC trace of the reaction mixture after assembly of the capsids by dialysis. The peak at 1.2 ml corresponds to 28 nm capsids, the 555 nm-absorbance shows that the capsid protein-AF555 conjugate is present in the capsids.

Capsid assembly

Self-assembly of the functionalized capsid protein was performed by 18 hour dialysis of the crude reaction mixture to a slightly acidic buffer (pH 5.0, 50 mM NaOAc; 1 M NaCl; 10 mM $CaCl_2$), which induces the formation of 28 nm sized spherical particles[3,4]. FPLC size exclusion analysis on a Superose 6 column showed an absorption peak at 280 nm at an elution volume of 1.2 ml, indicating the formation of 28 nm-sized capsids. The overlapping absorbance at 555 nm indicated the presence of Alexa dye in the capsids.

Transmission electron microscopy

An FPLC sample of the 1.2 ml peak was loaded on a TEM-grid, which was subsequently stained with 0.2% uranyl acetate in water. Analysis of the grid clearly shows the presence of spherical particles with a size of approximately 28 nm, the expected size for virus capsids.

Flow cytometry of glycan labeling

Cell culture procedure

Invasive and metastatic human melanoma cells (MV3)[5] were maintained in culture medium RPMI 1640, containing 10% fetal calf serum, penicillin/streptomycin (each 50U/ml) in a 5% CO_2 water-saturated atmosphere.

Cell surface azide labeling

MV3 cells were cultured for 6 days in the absence or presence of Ac_4ManNAz (50 µM). Medium and compound change was performed after 3 days. For live-cell labeling, cells were detached using EDTA (1 mM), washed and centrifuged three times (PBS, 300 x G, 5 min, 4 °C), resuspended in PBS and incubated in BCN-biotin **8** (60 µM), DIBO-biotin (60 µM), or buffer (1 h, 20 °C), washed three times (PBS, 300 x G, 2 min, 4 °C), resuspended in ice-cold PBS containing Alexa Fluor 488-conjugated streptavidin (5 µg/ml, Invitrogen; final volume 200 µl). After incubation (30 min, 4 °C), cells were washed three times, resuspended in PBS (200 µl, 4 °C) for further cell-function studies.

Flow cytometry

Flow cytometry was performed on a BD Biosciences FACS-Calibur flow cytometer using the 488 nm argon laser and data were analyzed with FCS Express version 3 research edition (De Novo Software, Los Angeles, CA). Per sample, $2x10^4$ morphologically intact cells were analyzed in the presence of propidium idodide (2.5 µg/ml).

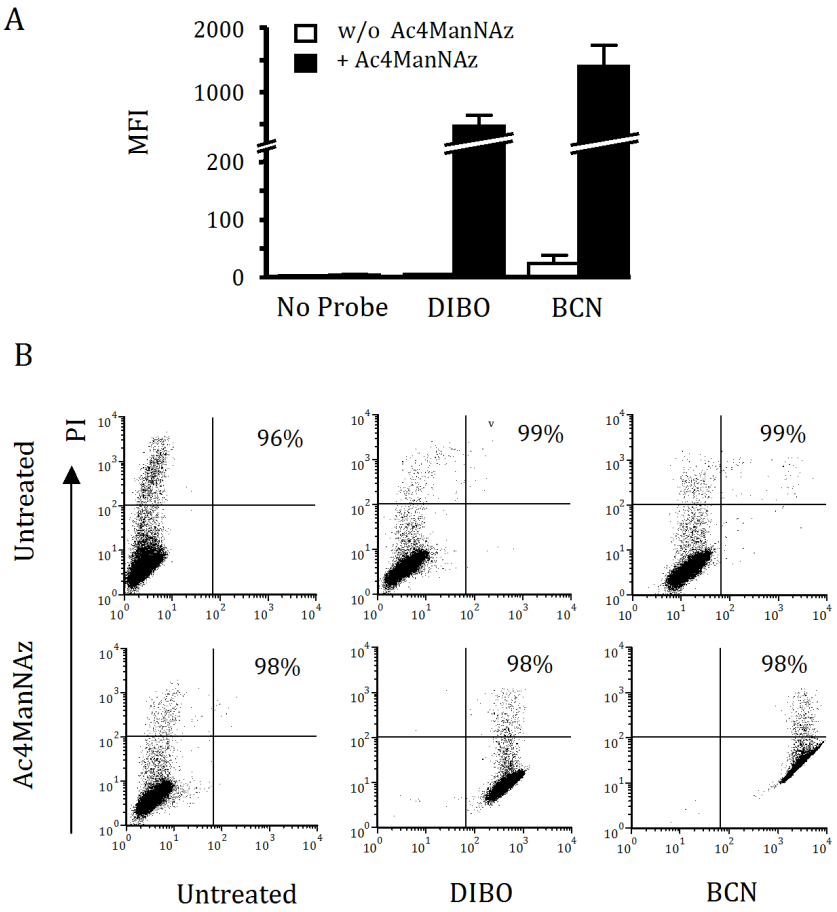

Fluorescence intensities and cell viability after cell labeling with Ac_4ManNAz and detection with DIBO- or BCN-biotin and secondary Alexa Fluor 488-conjugated streptavidin. (A) Mean intensities for green fluorescence (Alexa Fluor 488) and standard deviations (SD) from four independent experiments. (B) Intact cell viability after glycan labeling. Green fluorescence (Alexa Fluor 488) and propidium iodide (PI) label. Numbers indicate the percentage of PI-negative, viable cells.

Procedure for confocal microscopy and 3D imaging of glycan redistribution during invasive cell migrations

For confocal microscopy, azido-labeled cells were resuspended in normal culture medium, transferred to a 6-well plate and incubated for 30 min at 37 °C. Life cell imaging of MV3 cells was performed on a Olympus FV1000 confocal laser scanning microscope using excitation at 488 nm and emission detection of 520/50 nm.

Distribution studies of azido sialic acids were performed in 3D cell migration assays. Labeled MV3 cells were incorporated into 3D collagen I lattices and incubated for 90 min at 37°C, subsequently fixed with paraformaldehyde (4% in 0.1 M phosphate buffer) for 30 min at 37 °C and washed three times (PBS). Finally F-actin was stained with phalloidin Alexa Fluor 568 (Invitrogen, 2 U/ml) and nucleus with DAPI (Roche Diagnostics, 2,5 µg/ml).
Imaging of MV3 cells was performed as described above, using an additional excitation at 559 nm and emission detection of 647 nm and excitation at 405 nm and emission detection of 422 nm.

Pixel densitometry

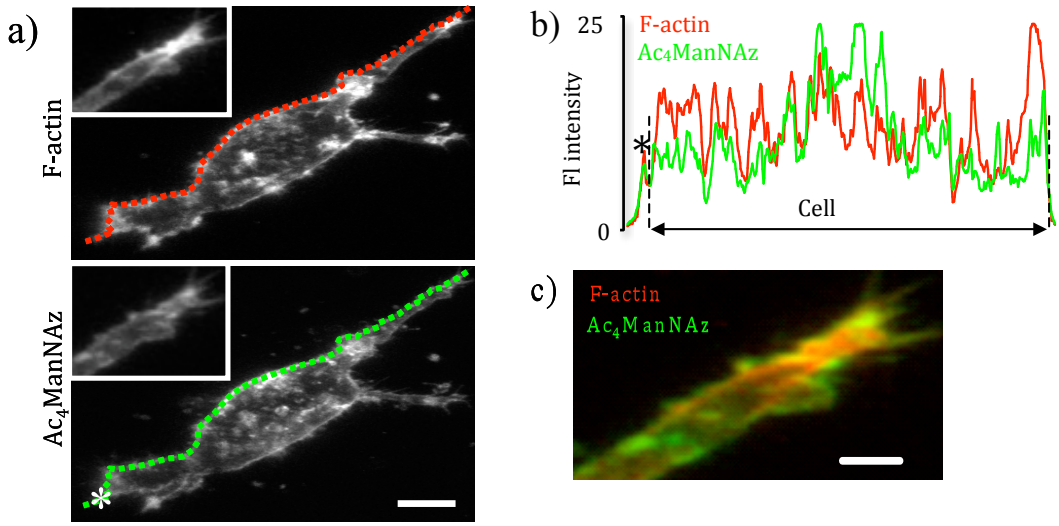

Intensity measurements of sialic acid and F-actin distribution at the cell surface. a) Region of interest for densitometric analysis. Bar 2 µm. b) Fluorescence intensity for sialic acid and F-actin from the leading to trailing edge. c) Two-channel detail of the leading pseudopod, revealing partial colocalization (yellow) in the sub-micron range. Asterisk, sialic acid containing deposited cell surface material. Bar 2 µm.

Literature references

[1] Minten, I. M., Hendriks, L. J. A., Nolte, R. J. M. & Cornelissen J. J. L. M. Controlled encapsulation of multiple proteins in virus capsids. *J. Am. Chem. Soc.* **131**, 17771 (2009).

[2] Link, A. J. & Tirrell, D. A. Reassignment of sense codons in vivo. *Methods* **36**, 291–298 (2005).

[3] Verduin, B. J. M. The preparation of CCMV-protein in connection with its association into a spherical-particle. *FEBS Lett.* **45**, 50–54 (1974).

[4] Comellas-Aragones, M., Engelkamp, H., Claessen, V. I.; Sommerdijk, N., Rowan, A. E., Christianen, P. C. M., Maan, J. C., Verduin, B. J. M., Cornelissen, J. J. L. M. & Nolte, R. J. M. *Nat. Nanotechnol*. **2**, 635 (2007).

[5] Maaser, K. *et al.*, "Functional hierarchy of simultaneously expressed adhesion receptors: integrin alpha2beta1 but not CD44 mediates MV3 melanoma cell migration and matrix reorganization within three-dimensional hyaluronan-containing collagen matrices," *Mol. Biol. Cell*. **10**, 3067 (1999).